SSRG International Journal of Electrical and Electronics Engineering
ISSN: 2348-8379/ https://doi.org/10.14445/23488379/IJEEE-V11I9P130

Volume 11 Issue 9, 333-343, September 2024

Original Article

An Efficient Grid Integrated Hybrid Renewable Energy System with Battery Storage Using SEPIC Converter

E. Immanuvel Bright[1]*, N. Pavithran[2], N. Rathika[3], M. Gnana Sundari[4], M. Balasubramanian[5], Kannan Kaliappan[6]

[1,2]*Department of Electrical and Electronics Engineering, Erode Sengunthar Engineering College, Tamilnadu, India.*
[3]*Department of Electrical and Electronics Engineering, Mahendra Institute of Technology, Tamilnadu, India.*
[4]*Department of Electrical and Electronics Engineering, Government College of Engineering, Bodinayakanur, Tamilnadu, India.*
[5]*Department of Electrical and Electronics Engineering, Government College of Engineering, Tirunelveli, Tamilnadu, India*
[6]*Department of Electrical and Electronics Engineering, Sreenidhi Institute of Science and Technology, Hyderabad, Telangana, India.*

[1]*Corresponding Author : immanuvelbright12@yahoo.com*

Received: 14 July 2024 Revised: 16 August 2024 Accepted: 14 September 2024 Published: 28 September 2024

Abstract - *The two most promising energy sources that are readily available in our nation are solar and wind, which help to protect the environment while simultaneously boosting the nation's economic well-being. The design and operation of a grid-connected hybrid energy source utilizing solar, wind and battery is demonstrated in this work. The proposed work was incorporated with the SEPIC converter due to its high voltage gain and efficiency with reduced ripple current, which is regulated by the PI controller. Moreover, the PWM generator is employed to produce pulses for the operation of the SEPIC converter. Three-phase VSI is utilized to convert the DC link voltage to AC to distribute power to the grid system. An AC output voltage is produced by a wind energy system based on a Doubly Fed Induction Generator (DFIG); through the use of a PWM rectifier, AC voltage is converted to DC effectively. The additional energy obtained from the hybrid PV/wind system is efficiently stored in the battery system, and an integrated battery converter allows the battery to be charged and discharged according to the battery needs. In the event of power unavailable from the wind and PV, the stored energy in the battery is utilized to distribute power to the grid system. The overall proposed system is applied in MATLAB/Simulink to validate the prominence of developed work, and it is contrasted with the other conventional topologies. By utilizing the developed SEPIC converter, low THD of 2.83%, high efficiency of 93.8% and high voltage gain of 1:8.9 are attained.*

Keywords - *3Φ VSI, Battery system, HRES, MATLAB/Simulink, PI controller, PV/wind, SEPIC converter.*

1. Introduction

With the current surge in energy demand and the shift to a low-carbon economy, innovative technology and services in the energy sector are more important than ever [1]. The two biggest global problems are extremes in temperature and greenhouse radiation. RES is undoubtedly going to be extremely important in the pursuit of a carbon-free society [2, 3].

Variable RES like solar energy, wind energy, and tidal energy are utilized as a remedy to minimize the harmful consequences of the reasons mentioned above because of their sustainability, cleanliness, and environmental friendliness [4, 5]. The present objective is to reduce emissions due to more dispersed generation and the power industry's growing importance. Due to environmental harm and growing fossil fuel consumption, eco-friendly RES have become more widespread [6].

The HRES, which blends several RES, is becoming more and more well-liked. In order to combat climate change, photovoltaic and wind renewable systems are essential in laying the path towards sustainable development and energy conservation [7, 8]. With regard to wind and photovoltaic power generation, the proposed approach is complementary to the HRES concept. For wind power production, DFIG based WECS is the most favourable solution [9].

This is because, in comparison to other energy conversion systems on the market, it provides a number of unique advantages. The primary concern is the dynamic response of DFIG to transients in grid voltage [10, 11]. Predicting the dynamic behaviour of PV power systems is difficult due to their nonlinear structure and reliance on external factors like sun irradiance and ambient temperature [12]. In solar power generation systems, a converter is required to convert the low-voltage PV system and high-voltage DC connection [13].

Boost [14], Buck, Boost [15], and Cuk [16] are the converters that are most frequently used in photovoltaic applications. These converters have low-order systems, high efficiency, and simplicity due to their Boost and Buck topologies. However, its limited output voltage flexibility limits its use, whereas the Boost converter only raises the voltage, the Buck converter decreases it, and it has high voltage stress [17, 18].

The Cuk converter steps up and down the voltage while producing a continuous input current [19]. However, the system's performance is limited by ripple current at the input and a high implementation complexity [20]. The suggested work created a SEPIC converter for PV voltage boosting in order to address the deficiency. In order to address the transient problems and produce a stabilized AC output voltage, the suggested solution uses a PI controller. For PV-wind systems to produce continuous electricity, especially when functioning as a stand-alone system, storage units (batteries) must be integrated in order to offset the intermittent nature of energy produced, which is utilized in this work.

2. Literature Review

Ahmad Aziz al Alahmadi et al. (2021) have developed RES based PID controllers for grid systems. This controller shows the stabilized power with high performance. However, poor settling time and overshoot issues are obtained by utilizing this control topology.

Octavian Cornea et al. (2020) have proposed a switched inductor hybrid converter for the HRES system. The converter provides a higher voltage conversion ratio and minimized ripple currents. Nevertheless, this technique faces challenges like power consumption, conduction losses and poor stability.

Mostafa et al. (2022) have implemented three port converters for PV and battery systems. The efficiency of the converter has remained high even in varying operating conditions. Despite this, the developed converter has high switching stress owing to the high component count.

Elham Amiri et al. (2020) presented a high boost-up multi-input converter for an HRES-fed grid system. High efficiency with high voltage gain is attained due to soft switching conditions, and it does not require additional components. However, it has higher magnetic losses due to the addition of a coupled inductor. In order to overcome the above stated challenges, the contributions of this paper are exemplified below,

- A hybrid RES with a battery system is employed to constantly deliver electricity to the grid.
- The SEPIC converter is implemented to boost the low voltage obtained from the PV system.
- Additional energy that occurs from the hybrid RES system is effectively stored in the battery system.

3. Proposed Modelling

An environmentally friendly and sustainable electric power generation that is self-sufficient through the use of HRES, such as solar and wind. When the HRES power supply is insufficient, the developed system energizes the grid with its stored excess energy, providing a continuous power supply regardless of the weather. The grid-connected system's balanced power flow is guaranteed by the converter and control method integration. The proposed work integrated with the SEPIC converter and PI controller to increase the voltage attained from the PV system, and the controller makes it easier to manage the SEPIC while enhancing the transient response effectively.

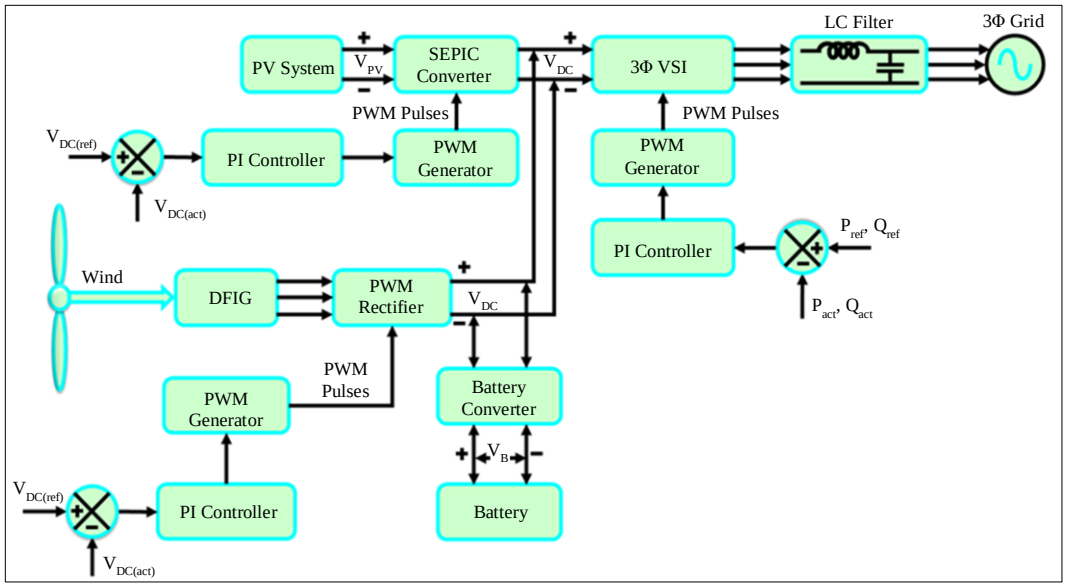

Fig. 1 HRES with energy management system

SEPIC converter is used to improve the low output of PV to match a needed supply for the grid system, which is controlled by the PI controller. On the other hand, the PWM rectifier is used to convert the AC supply from the DFIG based wind system, and the PI controller manages it. Subsequently, HRES output is fed to the DC link, and three-phase VSI is utilized to transform the DC supply into AC to deliver power to the grid system. Furthermore, the battery system is employed to store additional energy attained from the hybrid RES system, and the battery converter is employed to charge or discharge according to battery needs. During peak time, stored energy in the battery offers power back to the grid system. Thereby, adequate power is delivered to the grid.

3.1. Modelling of PV System

PV systems generate clean energy by absorbing sunlight and converting it into electricity. The circuit of one-diode equivalent is represented in Figure 2. The primary current equation is given as follows:

$$I = I_{pvcell} - I_{ocell}\left[exp\frac{(qv)}{akT} - 1\right] \quad (1)$$

$$I = I_{pv} - I_0\left[e\frac{(v+R_S.I)}{\propto V_k} - 1\right] - \frac{(v+R_S.I)}{R_p} \quad (2)$$

Where, q specifies electron charge, V_k indicates thermal voltage, I_{pv} denotes the photocurrent, T indicates the temperature of a cell, R_s represents the series resistance, I_0 indicates the cell saturation of dark current, $\propto$ illustrates the ideality factor, and R_p shunt resistance.

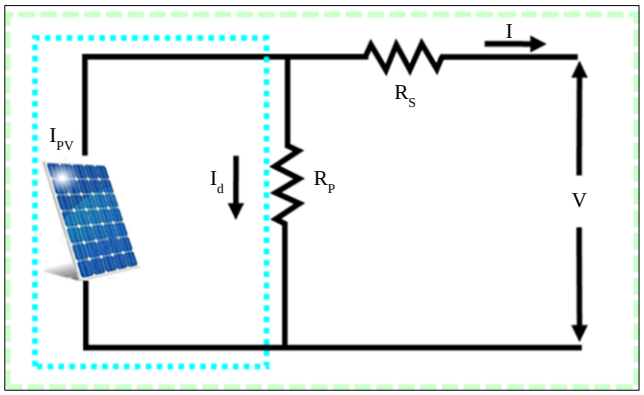

Fig. 2 Equivalent circuit of PV system

PV current is influenced by radiation, temperature, and the number of arrays in the PV panel. Equation (2) consequently turns into,

$$I = I_{pv} - I_0\left[exp\frac{(v+R_S.I)q}{\propto kT.Ns} - 1\right] - \frac{(v+R_S.I)}{R_p} \quad (3)$$

Where, $N_s$indicates a series of connected cells.

The SEPIC converter is used to improve the voltage received from PV, as explained below.

3.2. Modelling of SEPIC Converter

Depending on the duty cycle, the SEPIC, which is seen in Figure 3, functions as a boost or buck DC converter. The duty cycle of MOSFET is changed to increase or reduce the output voltage of the SEPIC converter. SEPIC uses energy exchange between the inductors and capacitors to transform a voltage from one source to another.

Switch S_1, which is usually a transistor, regulates the quantity of energy transferred. This converter contains a switch S_1, two capacitor(C_a, C_b), 2 inductor (L_a, L_b) and a diode D, respectively.

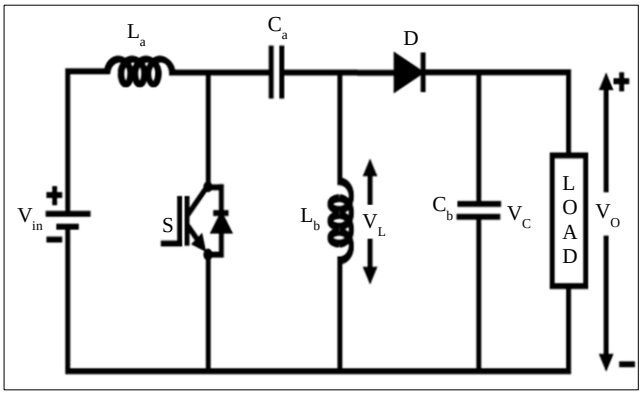

Fig. 3 Proposed SEPIC converter circuit diagram

Considering average voltages, the following expression can be expressed:

$$V_{in} = V_{La} + V_{Ca} + V_{Lb} \quad (4)$$

Given that V_{Ca} the average voltage is equal to V_{in},

$$V_{La} = V_{Lb} \quad (5)$$

The sum of the average currents is as follows.

$$I_{D1} = I_{La} - I_{Lb} \quad (6)$$

Mode 1 (ON state): When switch S_1 is ON, current in the inductor(L_a, orI_{La}) increases during the current in the inductor L_b, orI_{Lb}, becomes more negative. The input source is the source of the current I_{La}. Thus, instantaneous voltage V_{La} is equal to V_{in} and voltage V_{Lb} is equal to V_{Ca} when S_1 is closed. Subsequently, the opening of capacitors C_a and D results in an increase in the amount of energy stored in L_b and a magnitude of current inI_{Lb}.

Mode 2 (OFF state): The diode functions forward biassed when the switch is in the off position, and the output receives energy from the inductor L_a. when it charges the capacitor C_a as specified in Figure 4(b).

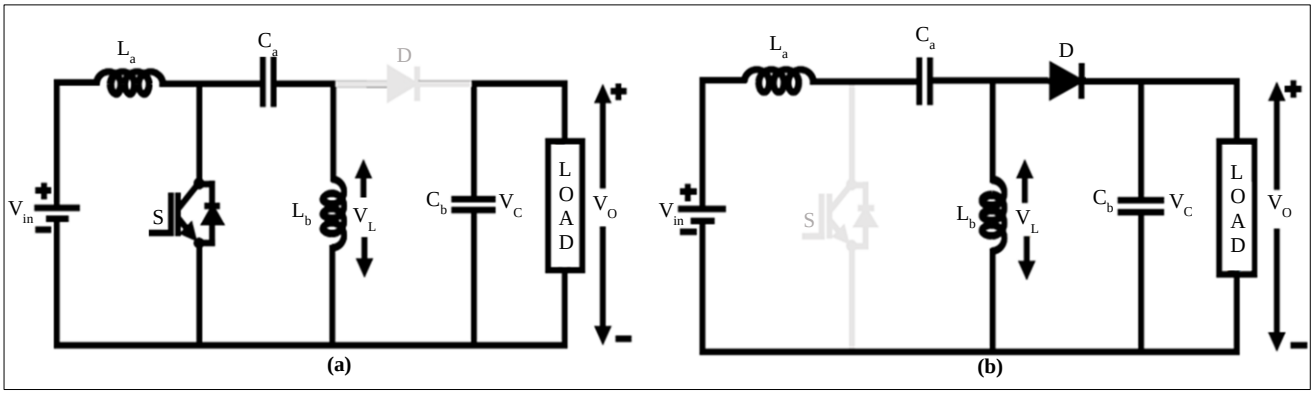

Fig. 4 Modes of operation (a) Mode 1, and (b) Mode 2.

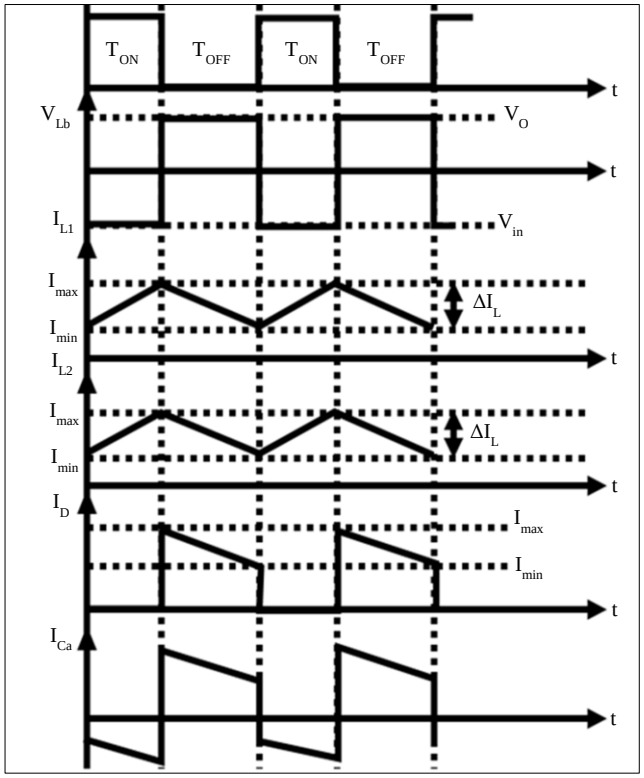

Fig. 5 Waveform for the SEPIC converter

3.2.1. Analysis of SEPIC converter

The following formulas constitute the basis of the SEPIC converter design.

The highest duty cycle is specified as,

$$D_{max} = \frac{V_{out}+V_D}{V_{in(min)}+V_{out}+V_D} \quad (7)$$

The minimum duty cycle is shown as,

$$D_{min} = \frac{V_{out}+V_D}{V_{in(max)}+V_{out}+V_D} \quad (8)$$

Given that the ripple current flowing through inductorsL_a,L_b is equal,

$$\Delta I_L = I_{out} \times \frac{V_{out}}{V_{in(min)}} \times 40\% \quad (9)$$

The value of the inductor is computed as,

$$L_a = L_b = L = \frac{V_{in(min)}}{\Delta I_L \times f_{sw}} \times D_{max} \quad (10)$$

The output capacitor is given as,

$$C_b \geq \frac{I_{out} \times D_{max}}{V_{ripple} \times 0.5 \times f_{sw}} \quad (11)$$

Consequently, the duty cycle range, inductorsL_a,L_b and capacitorsC_a, C_b are determined using the formulas mentioned above.

3.3. DFIG Based Wind System Modelling

3.3.1. Modelling of Wind Turbine

A collection of devices utilized to transform wind energy into electrical power is called a wind turbine. The wind turbine's mechanical output power is provided by,

$$P_m = \frac{1}{2}\rho\pi R^2 C_p(\alpha,\beta) {v_w}^2 \quad (12)$$

$$\alpha = \frac{\omega_t}{v_w} R \quad (13)$$

Where, C_p represents power coefficient function, α specifies tip speed ratio, ρ refers to the air density, β indicates blade pitch angle,v_w denotes wind speed and$\omega_t$indicates the angular speed of the rotor.

3.3.2. Modelling of DFIG

A DFIG is comprised of a series of windings that attach to a three phase transformer or a three phase shielded winding within the stator. Its stator is equipped with slip rings that are

connected to a grid through shielded windings or three phase transformers.

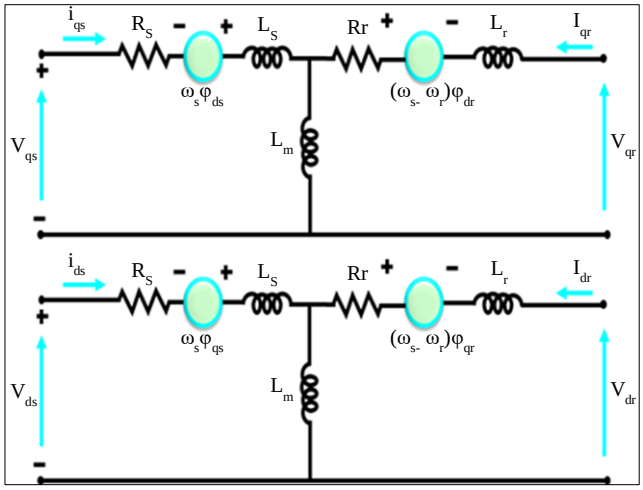

Fig. 6 DFIG based DQ frame reference theory

The subsequent equation gives the d−q reference of a DFIG:

$$\begin{cases} V_{ds} = R_s I_{ds} + \frac{d}{dt}\varphi_{ds} - \omega_{ds} - \omega_s \varphi_{qs} \\ V_{qs} = R_s I_{qs} + \frac{d}{dt}\varphi_{qs} - \omega_s \varphi_{dr} \\ V_{dr} = R_r I_{dr} + \frac{d}{dt}\varphi_{dr} - (\omega_s - \omega_r)\varphi_{qr} \\ V_{qr} = R_r I_{qr} + \frac{d}{dt}\varphi_{dr} - (\omega_s - \omega_r)\varphi_{qr} \end{cases} \quad (14)$$

The following equation states the rotor flux and stator,

$$\begin{cases} \varphi_{ds} = L_s I_{ds} + L_m I_{dr} \\ \varphi_{qs} = L_s I_{qs} + L_m I_{qr} \\ \varphi_{dr} = L_s I_{dr} + L_m I_{ds} \\ \varphi_{qr} = L_r I_{qr} + L_m I_{qs} \end{cases} \quad (15)$$

The following equation illustrates the torque equation of DFIG,

$$T_{em} = \frac{3}{2} p \frac{L_m}{L_r} \left(\varphi_{ds} I_{qr} - \varphi_{qs} I_{qr}\right) \quad (16)$$

The following equation defines the rotor active power,

$$P_r = \frac{3}{2}(V_{dr} I_{dr} - V_{qr} I_{qr}) \quad (17)$$

Moreover, the DFIG generated power is AC, which is turned into DC by adopting a PWM rectifier. Subsequently, the output from the wind energy and converter is delivered to the DC link. Three phase inverter is utilized for transforming DC into AC for distributing power to the grid system, and it is regulated with the assistance of a PI controller, as discussed below.

3.4. Modelling of PI controller

The PI controller, in this context, is to regulate an output of VSI to maintain desired performance despite disturbances or variations in load.

The following equation is defined as voltage error V_n

$$V(n) = V*(n) - V(n-1) \quad (18)$$

$$(n) = I(n-1) + K_p[V(n) - V(n-1)] + K_i V(n) \quad (19)$$

The reference grid currents direct as well as quadrature axis modules are given as,

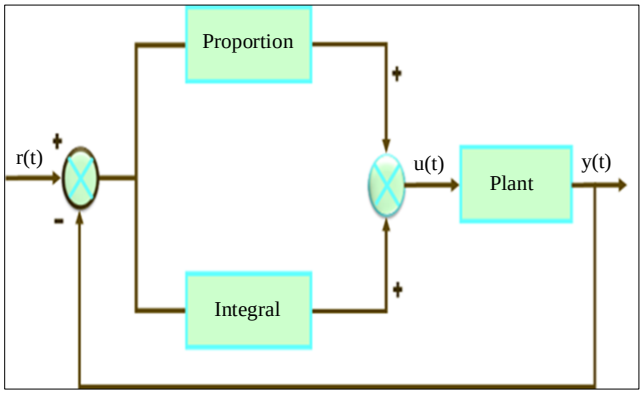

Fig. 7 Structure of PI controller

$$I_d = \left(K_p + \frac{K_i}{s}\right) * (V^*_{DC} - V_{DC}) \quad (20)$$

$$I_q = \left(K_p + \frac{K_i}{s}\right) * \left(Q^*_{grid} - Q_{grid}\right) \quad (21)$$

Where, V^*_{DC}indicates DC link voltage, V_{DC}shows measured DC link voltage, $K_p$is the proportional gain, $K_i$denotes integral gain, $Q_{grid}$is measured grid reactive and Q^*_{gtid}represents reference grid reactive power. The battery system is employed to store additional power from the HRES and provide backup during an insufficient supply from the HRES system to the grid.

3.4.1. Modelling of Bidirectional Battery Converter

A bidirectional battery converter has two modes of operation: charging and discharging. In charging mode, the converter modifies the DC source's power. Furthermore, this procedure involves raising or lowering voltage to correspond with the battery requirements to supply the appropriate voltage and current levels required by the battery.

$$L_{buck} = \frac{(V_{DC} - V_{batt}) D_{buck}}{\Delta I_{Lf}} \quad (22)$$

$$C_{buck} = \frac{(1 - D_{buck}) V_{batt}}{8 L_{buck} \Delta V_{batt} f^2} \quad (23)$$

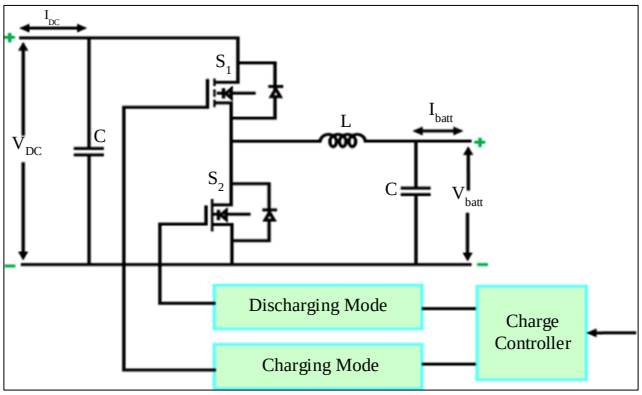

Fig. 8 Diagram of bidirectional battery converter

In discharging mode, the battery supplies its stored energy back to the DC source, which oversees the energy transfer to ensure that the battery discharges efficiently.

$$L_{boost} = \frac{V_{batt} D_{boost}}{\Delta I_{Lf}} \quad (24)$$

$$C_{boost} = \frac{V_{DC} D_{boost}}{R_0 \Delta V_{DCf}} \quad (25)$$

Therefore, the battery system attains better performance, and finally, the continual power supply is adequately delivered to the grid system.

4. Results and Discussion

This study offers a hybrid PV and wind system with a SEPIC converter for grid application. SEPIC converter gives high efficiency and voltage gain with reduced ripple current. The overall implemented work is applied in MATLAB/Simulink to validate the effectiveness of the proposed system. Furthermore, a developed topology is compared with other conventional converter approaches to show the prominence of the developed work and parameter specification is represented in Table 1, which is defined below.

Table 1. Parameter specification

PV and DFIG	
Parameters	**Ratings**
Open Circuit Voltage	12V
Peak Power	10Kw
Series Connected Solar Panel	36
Short Circuit Current	8.3A
No. of Turbine	1
Voltage	575V
Switching Frequency	10kHz
Power	10kW
SEPIC Converter	
Switching Frequency	$10kHz$
$C_{a,}C_b$	$4.7\mu F$
L_a, L_b	$1\ mH$

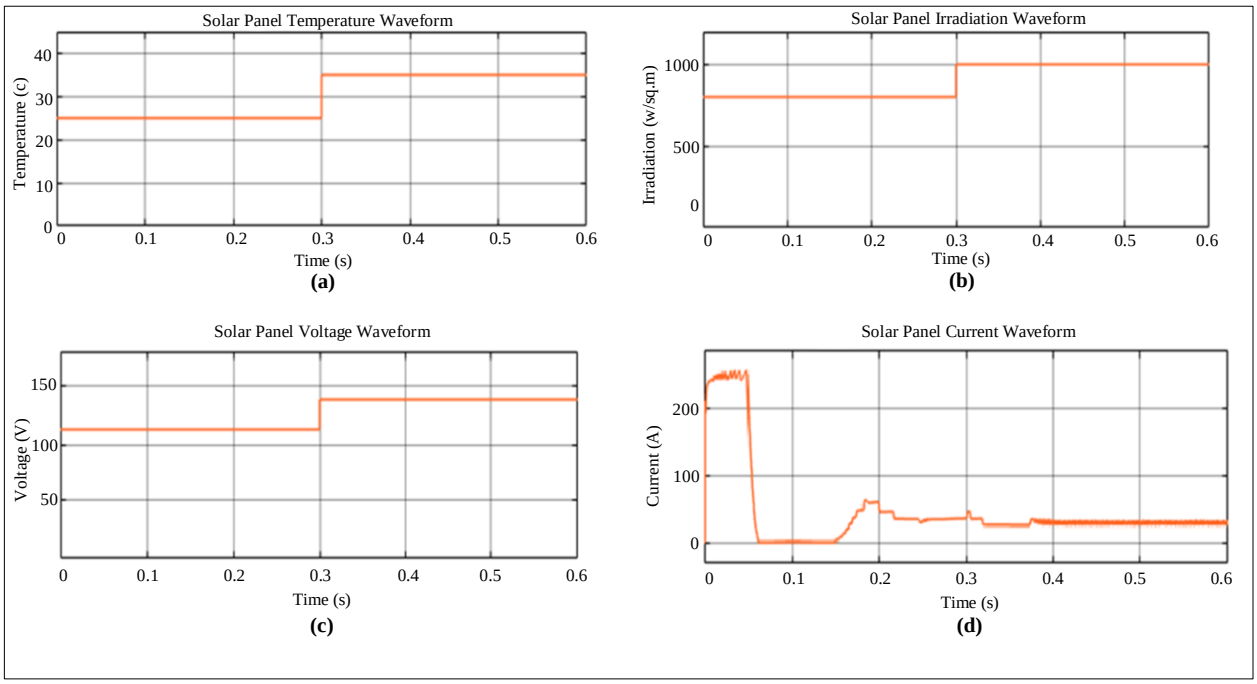

Fig. 9 Solar panel waveform

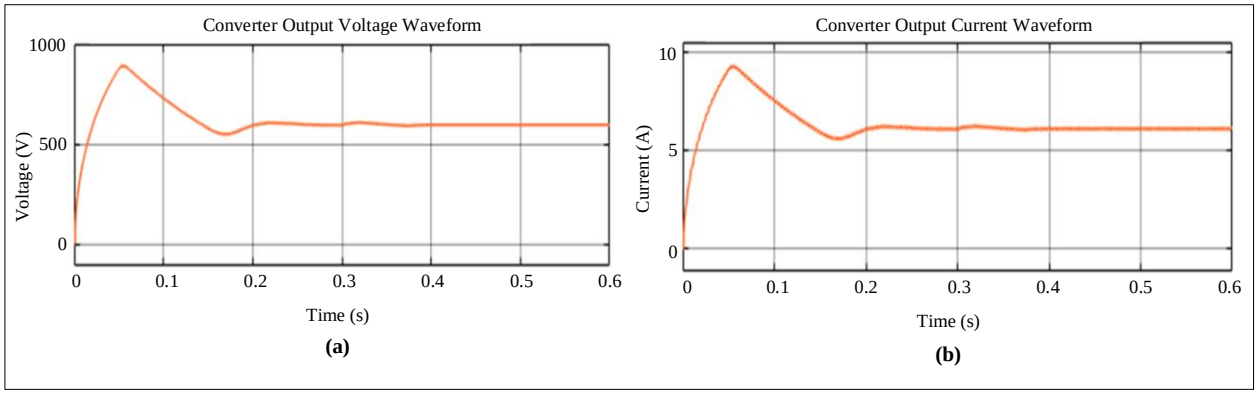

Fig. 10 Converter waveform (a) Voltage, and (b) Current.

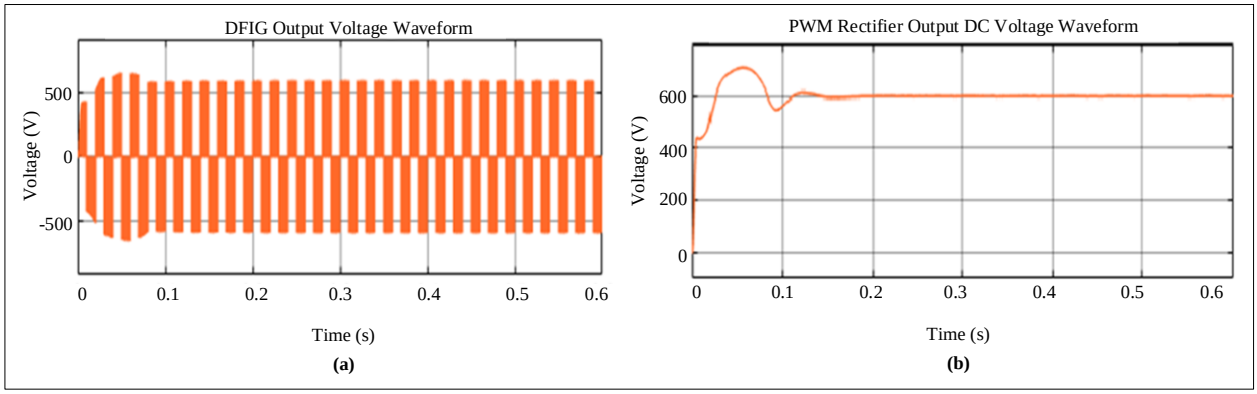

Fig. 11 (a) DFIG output voltage, and (b) PWM rectifier voltage waveform.

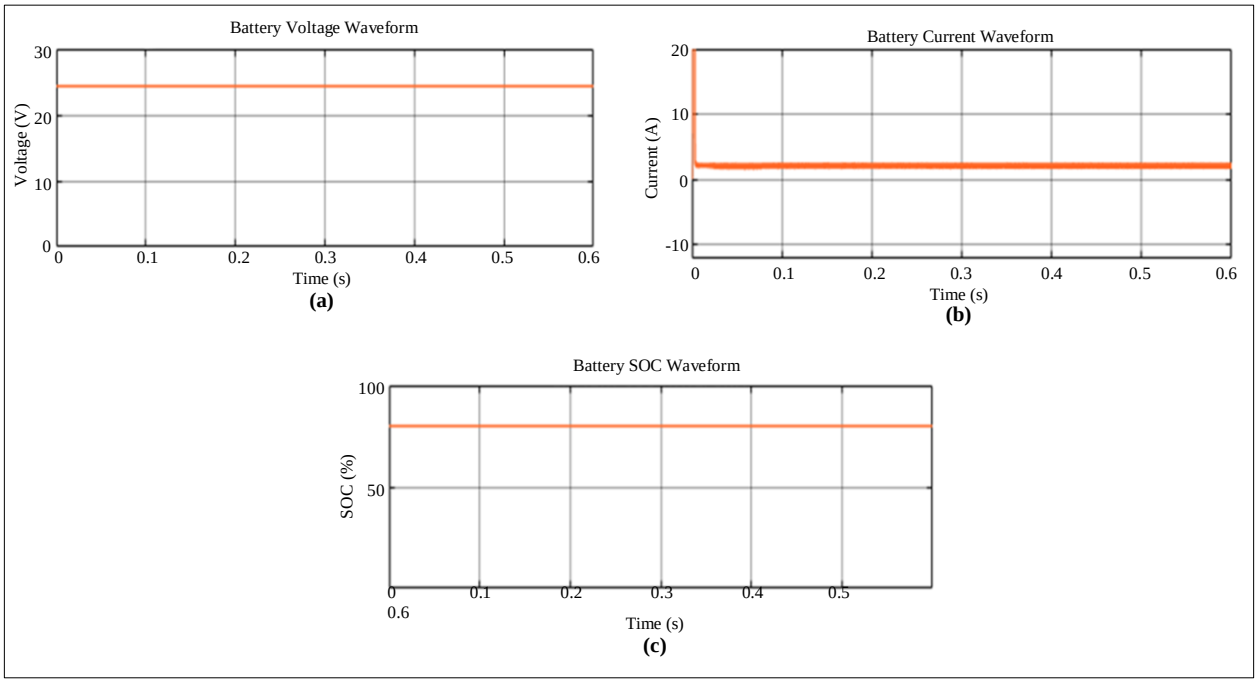

Fig. 12 Battery waveform (a) Voltage, (b) Current, and (c) SOC.

Solar panel waveform for implemented work is demonstrated in Figure 9, which analyzed that the temperature of the solar panel varies at certain periods of time, and it gets continually maintained at 35C after 0.3s as specified in Figure 9(a). Likewise, Figure 9(b) specifies that the irradiation of solar panels gets stabilized at 1000 (w/Sq.m) after 0.3s. Furthermore, the solar panel voltage oscillates before 0.3s, and it is continuously preserved at 140V after 0.3s, as specified in Figure 9(c).

The solar panel current shown in Figure 9(d) is evident that the current oscillates for a certain period of time, and after 0.4s, it is continually preserved at 20A. The SEPIC converter waveform is specified in Figure 10, which maintains the voltage continuously at 600V after oscillating for a certain period of time, as specified in Figure 10(a). Also, the converter current is represented in Figure 10 (b), which fluctuated highly initially and was constantly maintained at 7A after 0.5s. The waveform for the DFIG and PWM rectifier output voltage waveform is shown in Figure 11. From Figure 11(a), it is evident that the DFIG voltage is constantly maintained at 510V after 0.4s. Furthermore, the PWM rectifier output DC voltage fluctuated highly in the initial period. After 0.25s, output DC voltage is constantly sustained at 600V, as represented in Figure 11 (b). The battery waveform for the implemented work is exemplified in Figure 12, which shows that the battery voltage is continually stabilized at 25V, as stated in Figure 12(a). Likewise, the current oscillated and was constantly maintained at 3A, as indicated in Figure 12 (b). As represented in Figure 12(c), the SOC is constantly preserved at 75% in this work correspondingly.

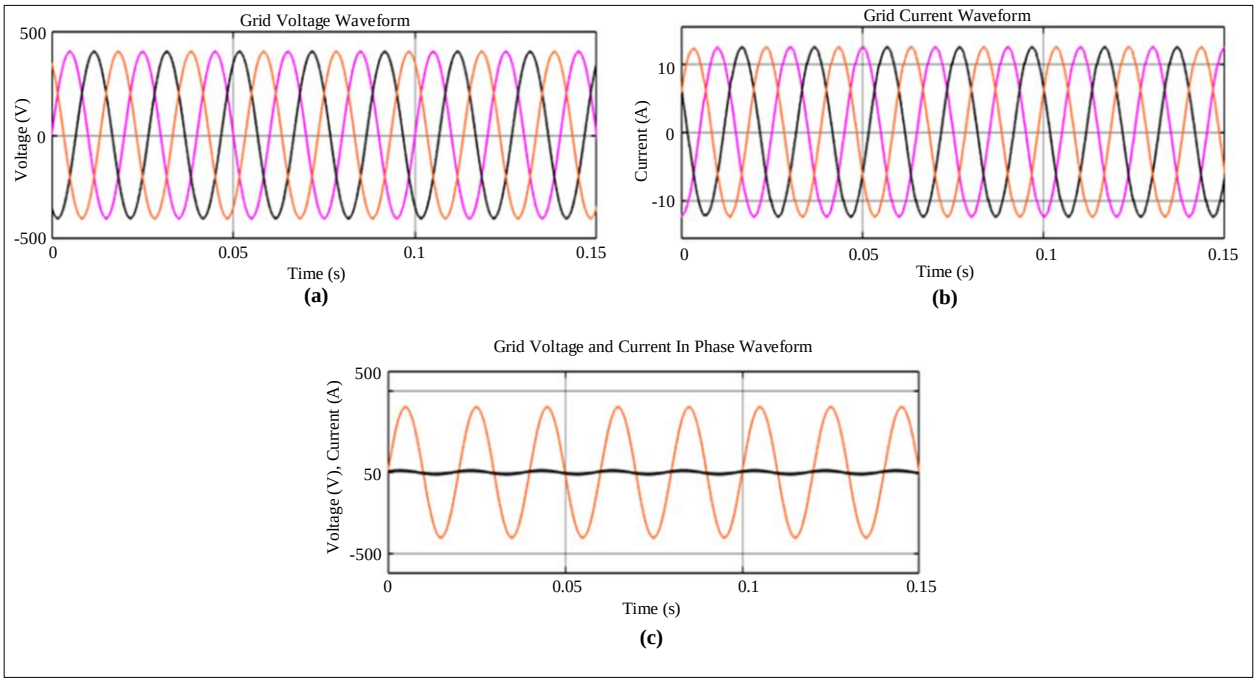

Fig. 13 Grid Waveform

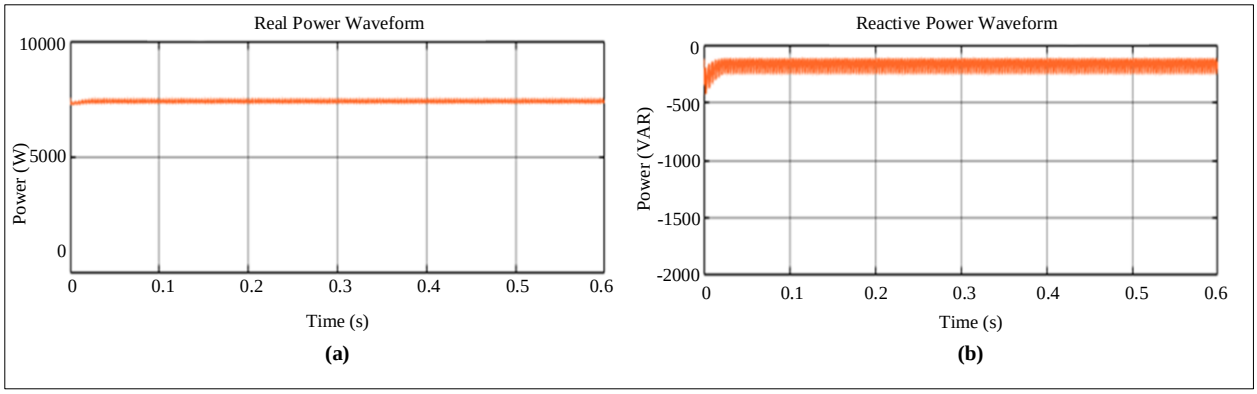

Fig. 14 (a) Real, and (b) Reactive power waveform.

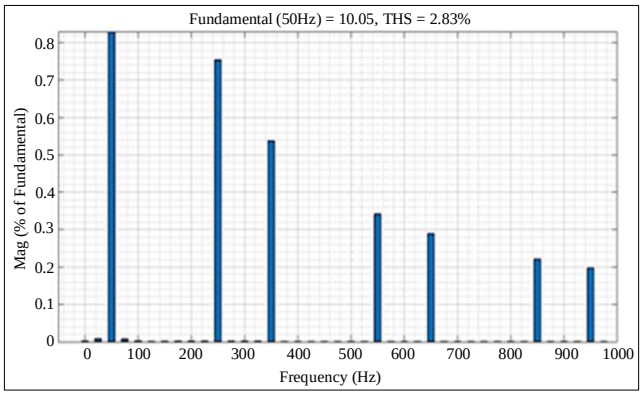

Fig. 15 THD waveform

Grid voltage and current waveform are represented in Figure 13. As specified in Figure 13(a), grid voltage gets continuously preserved at 400 to -400V. Similarly, the grid current is maintained stable at 11 to -11A, as exemplified in Figure 13(b). As stated in Figure 13(c), grid voltage and current are continuously preserved at 400V to -400V and 0A, respectively.

Figure 14 shows the waveforms for both real and reactive power. It is seen that the proposed system achieves stable real and reactive power, leading to improved system performance, as shown in Figure 14(a) and (b), respectively.

Figure 15 demonstrates the THD waveform for the developed work from the analysis that the proposed SEPIC converter achieves a THD value of 2.83%.

Table 2. Efficiency comparison

Converters	Efficiency (%)
Boost [21]	91.2
Buck-Boost [22]	92.4
Cuk [19]	88
SEPIC	93.8

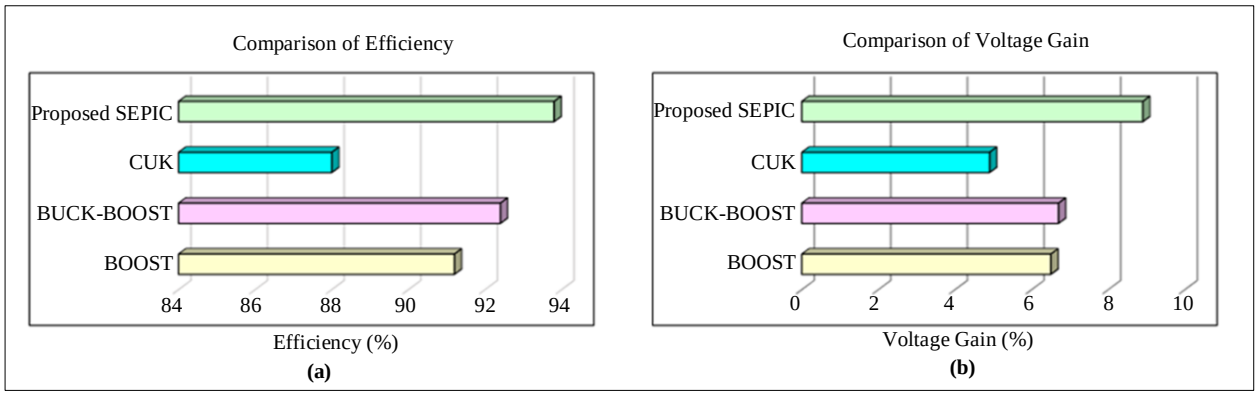

Fig. 16 Comparison of converter (a) Efficiency, and (b) Voltage gain.

The efficiency and voltage gain comparison with other conventional converters is represented in Figure 16. It is clear from Figure 16(a) and Table 2 that the developed SEPIC converter outperforms other topologies like Boost, Buck-Boost, and Cuk converter, achieving a high efficiency of 93.8%. Likewise, the SEPIC Converter is compared with the existing techniques to determine better voltage gain. As represented in Figure 16(b) and Table 3, the proposed converter obtains a higher voltage gain of 1:8.9 than the previous approaches.

Table 3. Comparison of voltage gain

Converters	Voltage Gain (%)
Boost [21]	1:6.5
Buck-Boost [22]	1:6.7
CUK [23]	1:4.9
Proposed Converter	1:8.9

The developed converter has a low THD value of 2.83% when compared to the other topologies, as demonstrated by the efficiency comparison graph of Figure 17 between the proposed SEPIC converter and other conventional converters such as Boost, Buck-boost, and Cuk converter.

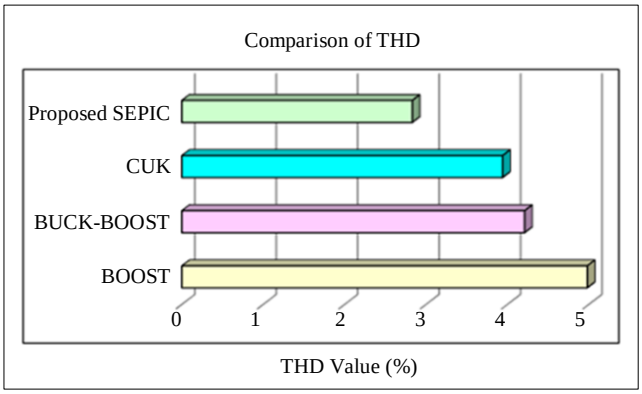

Fig. 17 Comparison of THD value

5. Conclusion

In this work, an efficient grid integrated hybrid PV and wind energy based DFIG system with battery storage using a SEPIC converter is proposed. The low output of the PV system is effectively raised with high efficiency with the aid of the SEPIC converter, which is also effectively regulated by the PI controller. Furthermore, by adopting the battery system, extra energy obtained from the hybrid PV/wind system is effectively stored, and an integrated battery converter enables the battery to be charged and discharged in accordance with the battery's needs. Stored energy is utilized during the lagging period of energy from the hybrid RES system. An entire system is implemented in MATLAB/Simulink to demonstrate the importance of developed work, and it is compared with other existing topologies to show the proposed system's performance. The comparison results illustrate that the proposed SEPIC converter achieved a low THD of 2.83%, high efficiency of 93.8% and high voltage gain of 1:8.9, respectively.

References

[1] Karan Doshi, and V.S.K.V. Harish, "Analysis of a Wind-PV Battery Hybrid Renewable Energy System for a DC Microgrid," *Materials Today: Proceedings*, vol. 46, pp. 5451-5457, 2021. [CrossRef] [Google Scholar] [Publisher Link]

[2] Pandav Kiran Maroti et al., "A New Structure of High Voltage Gain SEPIC Converter for Renewable Energy Applications," *IEEE Access*, vol. 7, pp. 89857-89868, 2019. [CrossRef] [Google Scholar] [Publisher Link]

[3] Xibeng Zhang et al., "Model Predictive and Iterative Learning Control Based Hybrid Control Method for Hybrid Energy Storage System," *IEEE Transactions on Sustainable Energy*, vol. 12, no. 4, pp. 2146-2158, 2021. [CrossRef] [Google Scholar] [Publisher Link]

[4] Sanghita Baidya, and Champa Nandi, "Green Energy Generation Using Renewable Energy Technologies," *Advances in Greener Energy Technologies*, pp. 259-276, 2020. [CrossRef] [Google Scholar] [Publisher Link]

[5] Muhammad Majid Gulzar et al., "An Innovative Converterless Solar PV Control Strategy for a Grid Connected Hybrid PV/Wind/Fuel-Cell System Coupled with Battery Energy Storage," *IEEE Access*, vol. 11, pp. 23245-23259, 2023. [CrossRef] [Google Scholar] [Publisher Link]

[6] Bhaskara Rao Ravada, Narsa Reddy Tummuru, and Bala Naga Lingaiah Ande, "Photovoltaic-Wind and Hybrid Energy Storage Integrated Multisource Converter Configuration-Based Grid-Interactive Microgrid," *IEEE Transactions on Industrial Electronics*, vol. 68, no. 5, pp. 4004-4013, 2020. [CrossRef] [Google Scholar] [Publisher Link]

[7] Md. Nafiz Musarrat, and Afef Fekih, "A Fault-Tolerant Control Framework for DFIG-Based Wind Energy Conversion Systems in a Hybrid Wind/PV Microgrid," *IEEE Journal of Emerging and Selected Topics in Power Electronics*, vol. 9, no. 6, pp. 7237-7252, 2021. [CrossRef] [Google Scholar] [Publisher Link]

[8] Ahmad Aziz Al Alahmadi et al., "Hybrid Wind/PV/Battery Energy Management-Based Intelligent Non-Integer Control for Smart Dc-Microgrid of Smart University," *IEEE Access*, vol. 9, pp. 98948-98961, 2021. [CrossRef] [Google Scholar] [Publisher Link]

[9] Muhammad Maaruf, Khalid Khan, and Muhammad Khalid, "Robust Control for Optimized Islanded and Grid-Connected Operation of Solar/Wind/Battery Hybrid Energy," *Sustainability*, vol. 14, no. 9, 2022. [CrossRef] [Google Scholar] [Publisher Link]

[10] Ali M. Eltamaly, M.S. Al-Saud, and Ahmed G. Abo-Khalil, "Dynamic Control of a DFIG Wind Power Generation System to Mitigate Unbalanced Grid Voltage," *IEEE Access*, vol. 8, pp. 39091-39103, 2020. [CrossRef] [Google Scholar] [Publisher Link]

[11] Abrar Ahmed Chhipa et al., "Modeling and Control Strategy of Wind Energy Conversion System with Grid-Connected Doubly-Fed Induction Generator," *Energies*, vol. 15, no. 18, 2022. [CrossRef] [Google Scholar] [Publisher Link]

[12] M. Pushpavalli, and N.M. Jothi Swaroopan, "KY Converter with Fuzzy Logic Controller for Hybrid Renewable Photovoltaic/Wind Power System," *Transactions on Emerging Telecommunications Technologies*, vol. 31, no. 12, 2020. [CrossRef] [Google Scholar] [Publisher Link]

[13] Balaji Chandrasekar et al., "Non-Isolated High-Gain Triple Port DC-DC Buck-Boost Converter with Positive Output Voltage for Photovoltaic Applications," *IEEE Access*, vol. 8, pp. 113649-113666, 2020. [CrossRef] [Google Scholar] [Publisher Link]

[14] Qun Qi, Davood Ghaderi, and Josep M. Guerrero, "Sliding Mode Controller-Based Switched-Capacitor-Based High DC Gain and Low Voltage Stress DC-DC Boost Converter for Photovoltaic Applications," *International Journal of Electrical Power & Energy Systems*, vol. 125, 2021. [CrossRef] [Google Scholar] [Publisher Link]

[15] Mahmoud Dhimish, and Nigel Schofield, "Single-Switch Boost-Buck DC-DC Converter for Industrial Fuel Cell and Photovoltaics Applications," *International Journal of Hydrogen Energy*, vol. 47, no. 2, pp. 1241-1255, 2022. [CrossRef] [Google Scholar] [Publisher Link]

[16] Hossein Gholizadeh et al., "Design and Implementation of a New Cuk-Based Step-Up DC-DC Converter," *Energies*, vol. 14, no. 21, 2021. [CrossRef] [Google Scholar] [Publisher Link]

[17] Parham Mohseni et al., "Ultrahigh Voltage Gain DC-DC Boost Converter with ZVS Switching Realization and Coupled Inductor Extendable Voltage Multiplier Cell Techniques," *IEEE Transactions on Industrial Electronics*, vol. 69, no. 1, pp. 323-335, 2022. [CrossRef] [Google Scholar] [Publisher Link]

[18] Hakan Tekin, Kubra Bulut, and Davut Ertekin, "A Novel Switched-Capacitor and Fuzzy Logic-Based Quadratic Boost Converter with Mitigated Voltage Stress, Applicable for DC Micro-Grid," *Electrical Engineering*, vol. 104, pp. 4391-4413, 2022. [CrossRef] [Google Scholar] [Publisher Link]

[19] Khaled A. Mahafzah et al., "A New Cuk-Based DC-DC Converter with Improved Efficiency and Lower Rated Voltage of Coupling Capacitor," *Sustainability*, vol. 15, no. 11, 2023. [CrossRef] [Google Scholar] [Publisher Link]

[20] Jialin Luo et al., "Novel Cuk-Based Bridgeless Rectifier of WPT System with Wide Power Modulation Range and Low Current Ripple," *IEEE Transactions on Industrial Electronics*, vol. 69, no. 3, pp. 2533-2544, 2022. [CrossRef] [Google Scholar] [Publisher Link]

[21] Arafa S. Mansour, and Mohamed S. Zaky, "A New Extended Single-Switch High Gain DC-DC Boost Converter for Renewable Energy Applications," *Scientific Reports*, vol. 13, 2023. [CrossRef] [Google Scholar] [Publisher Link]

[22] Tohid Rahimi et al., "Design and Implementation of a High Step-Up DC-DC Converter Based on the Conventional Boost and Buck-Boost Converters with High Value of the Efficiency Suitable for Renewable Application," *Sustainability*, vol. 13, no. 19, 2021. [CrossRef] [Google Scholar] [Publisher Link]

[23] S.K. Janarthanan, and C. Kathirvel, "Optimized CUK Converter Based 1Φ Grid Tied Photovoltaic System," *Intelligent Automation and Soft Computing*, vol. 34, no. 1, pp. 33-50, 2022. [CrossRef] [Google Scholar] [Publisher Link]